

Microstructure and properties of carbon fiber sized with pickering emulsion based on graphene oxide sheets and its composite with epoxy resin

Cuicui Wang,^{1,2} Heyi Ge,^{1,2} Huashi Liu,^{1,2} Shuai Guo^{1,2}

¹Shandong Provincial Key Laboratory of Preparation and Measurement of Building Materials, University of Jinan, Jinan 250022, People's Republic of China

²School of Material Science and Engineering, University of Jinan, Jinan 250022, People's Republic of China

Correspondence to: H. Ge (E-mail: geheyi@sina.com)

ABSTRACT: The Graphene oxide (GO) sheets were used for preparing the epoxy resin Pickering emulsion. The particle size and the zeta potential of the Pickering emulsion were measured to evaluate its stability. The stable emulsion could be served as the film former of sizing agent for carbon fiber (CF). The effect of the Pickering emulsion stabilized by GO sheets on the properties of CF and the interfacial adhesion property of CF reinforced composite were investigated. Scanning electron microscopy (SEM) images showed that there existed a layer of sizing agent film with GO sheets evenly on the CF surface. Abrasion resistance and stiffness values of CF were tested and the results indicated that the sized CF conformed to the requirement of CF handleability. The interlaminar shear strength (ILSS) test indicated that the interfacial adhesion of the composite could be greatly improved. The fracture surfaces of CF composites were examined by SEM after ILSS tests. © 2015 Wiley Periodicals, Inc. *J. Appl. Polym. Sci.* 2015, 132, 42285.

KEYWORDS: fibers; graphene and fullerenes; nanotubes; phase behavior; surfactants; surfaces and interfaces

Received 20 January 2015; accepted 31 March 2015

DOI: 10.1002/app.42285

INTRODUCTION

Carbon fiber (CF) is widely used as reinforced material in composites, especially in advanced composites.^{1–5} However, the surface of CF exhibits inertness, and the interfacial adhesion between CF and resin matrix is generally very weak. For good bonding and stress transfer, CF is generally sized or coated with a thin polymer layer.^{6–8} Resin emulsion-stabilized chemical surfactants are usually used as film former of sizing agent. However, because of the thermodynamic instability of general emulsifier, the stability of emulsion would easily be affected by the external factors such as temperature, pH value and occur the phenomenon of stratification or precipitation, etc.⁹ Meanwhile, surfactant molecules could move freely and tend to assemble on the surface of sizing agent film and form a hydrophilic layer. Then the hydrophilic layer is liable to absorb water and damages the interfacial adhesion between CF and matrix. So the existence of excessive surfactants may influence the interfacial adhesion and water resistance of composites.¹⁰ Pickering emulsion indicates that emulsion is stabilized by solid particles instead of organic surfactants.^{11–13} In Pickering emulsion, fine solid particles adsorbed at the oil–water interface impede the coalescence of two droplets.^{14,15} Because the process of adsorption is irreversible, Pickering emulsion is very stable and could

reduce the dosage of chemical emulsifiers.^{16–19} More recently, some indications emerged on the fact that solid particle homogeneously dispersed in a polymer matrix or localized at the interfacial region could play a beneficial role on the fiber/matrix interfacial adhesion in several types of structural composites.^{20,21}

Graphene oxide (GO) sheets, an oxidized shape of graphene, have good handling characteristics and chemical reactivity in solution because of the intrinsic functional groups.²² Many reported studies about graphene and GO were utilized for preparation of polymeric nanocomposites, such as polyaniline nanostructures,²³ poly(methyl methacrylate) nanocomposites,²⁴ poly(vinyl alcohol) nanocomposites,²⁵ poly(styrene) nanocomposite.²⁶ In addition, GO as an effective fire retardant of epoxy resin was researched in detail.²⁷ Han²⁸ also reported the dispersion, mechanical, and crystallization properties of low-density polyethylene with graphene modified lipophilically. Studies on the wettability of GO showed that the water contact angle was in the range of 62–68°,^{29,30} much less than 90°, which demonstrated that GO was partially hydrophilic and tended to stabilize o/w emulsions because the particle surface resided more in water than in oil.³¹ In our precious work, Pickering emulsion type sizing agent stabilized by nano-SiO₂ for glass fiber was

Table I. Compositions of the Sizing Agents

| Material/sizing agents | Emulsifiers (g) | GO (g) | Resin (g) | Glycidylether (g) | Distilled water (g) |
|------------------------|-----------------|--------|-----------|-------------------|---------------------|
| SA-1 | 5 | 0 | 50 | 5 | 200 |
| SA-2 | 2.5 | 0.15 | 50 | 5 | 200 |
| SA-3 | 2.5 | 0 | 50 | 5 | 200 |

prepared.³² However, Pickering emulsion type sizing agent stabilized by GO sheets for CF has never been researched. Can the Pickering emulsion stabilized by GO sheets be used of CF sizing agent and then sized on the CF surface to improve the performance of interface bonding?

There is the reported work on the adding GO sheets aqueous suspension directly into CF sizing agent.³³ However, very few reports about Pickering emulsion stabilized by GO as CF sizing agent have been published. Furthermore, there are hardly any reported works on the microstructure and the properties of CF sized with Pickering emulsion based on GO sheets and its composite. The aim of this study was to prepare the stable Pickering emulsion and investigate its properties. The study further aimed at investigating the influences of the Pickering emulsion on the surface of CF and CF composite. For this purpose, the Pickering emulsion stabilized by GO sheets was prepared and the effects on CF and the composite were investigated in detail.

EXPERIMENTAL

Materials

Natural graphite flakes were supplied by Aladdin Industrial Corporation. Concentrated sulfuric acid (H_2SO_4), sodium nitrate ($NaNO_3$), potassium permanganate ($KMnO_4$), hydrogen peroxide (H_2O_2), were of analytical grade and purchased from Sinopharm Chemical Reagent (Shanghai, China). Epoxy resin E-51 (viscosity of 15 Pa·s, epoxy value of 0.48–0.54) and neopentyl glycol diglycidyl ether were supplied by Tianmao Chemical. Commercial available T700S CF (12 K) was supplied by Japan Toray. Emulsifiers [Span80, OP-10, and sodium dodecylbenzene sulfonate (SDBS)] and the hardener triethylenetetraamine (TETA) were homemade and purchased from Tianjin Guangfu Institute of Fine Chemical.

Preparation of the Pickering Emulsion Stabilized by GO and Sized CF

The GO sheets were synthesized according to the modified Hummers method as described in our previous reports.³⁴

The GO sheets stabilized Pickering emulsion was prepared by phase inversion emulsification method. A certain amount of epoxy resin (50 g), emulsifiers (OP-10/Span80/SDBS) (2.5 g), and neopentyl glycol diglycidyl ether (5 g) were added into the flask and blended by constant stirring until the mixture was homogeneous. The Next, the GO sheets aqueous suspension with the concentrations of 0.00075 g/mL was guttatim dripped into the above epoxy resin solution. Meanwhile, the solution was dispersed by a high shear dispersion homogenizer at a mixing speed of 9000 rpm. Finally, A Pickering emulsion containing about 20% solid content was obtained. In this work, the mass ratios of water/resin and OP-10/Span80/SDBS were fixed at 4 : 1 and 65 : 25 : 10, respectively. For comparison, Table I demonstrates the compositions of the sizing agents. During in the reaction process, the content and the concentration of materials were the optimized conditions for this experiment.

To remove the sizing agent coated on the commercial CF surface, T700 CF was refluxed in acetone for 36 h with a soxhlet apparatus, washed repeatedly with deionized water, and dried in vacuo at 100°C for 12 h.³⁵ The sizing agent was gained after the mixture was diluted to a 1.5% solid content with deionized water. A dipping method was used in the sizing process. The CF was immersed in the sizing agent for 30 s by use of a dip tank in conjunction with automatic processing equipment for continuous running of CF. Then the CF was dried at 100°C for 20 min.^{2,36} The procedure is vividly illustrated by Figure 1.

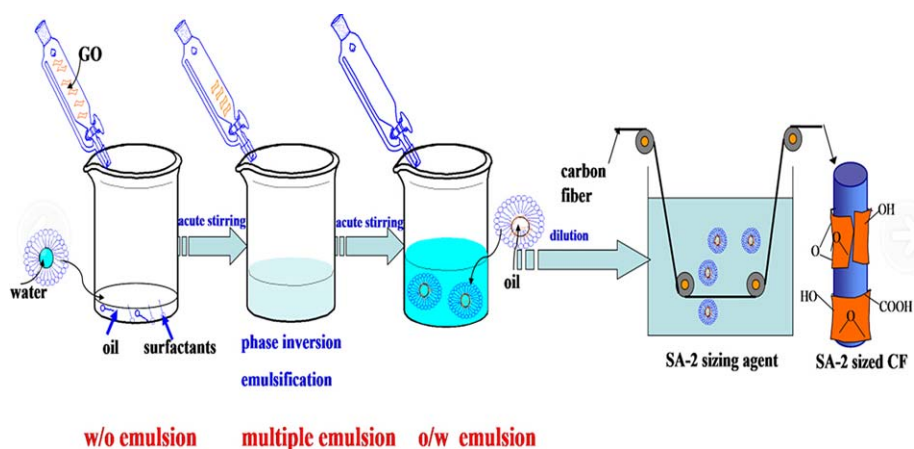


Figure 1. Schematic illustration of preparation of SA-2 sizing agent stabilized by GO sheets and the sized CF with SA-2 sizing agent. [Color figure can be viewed in the online issue, which is available at wileyonlinelibrary.com.]

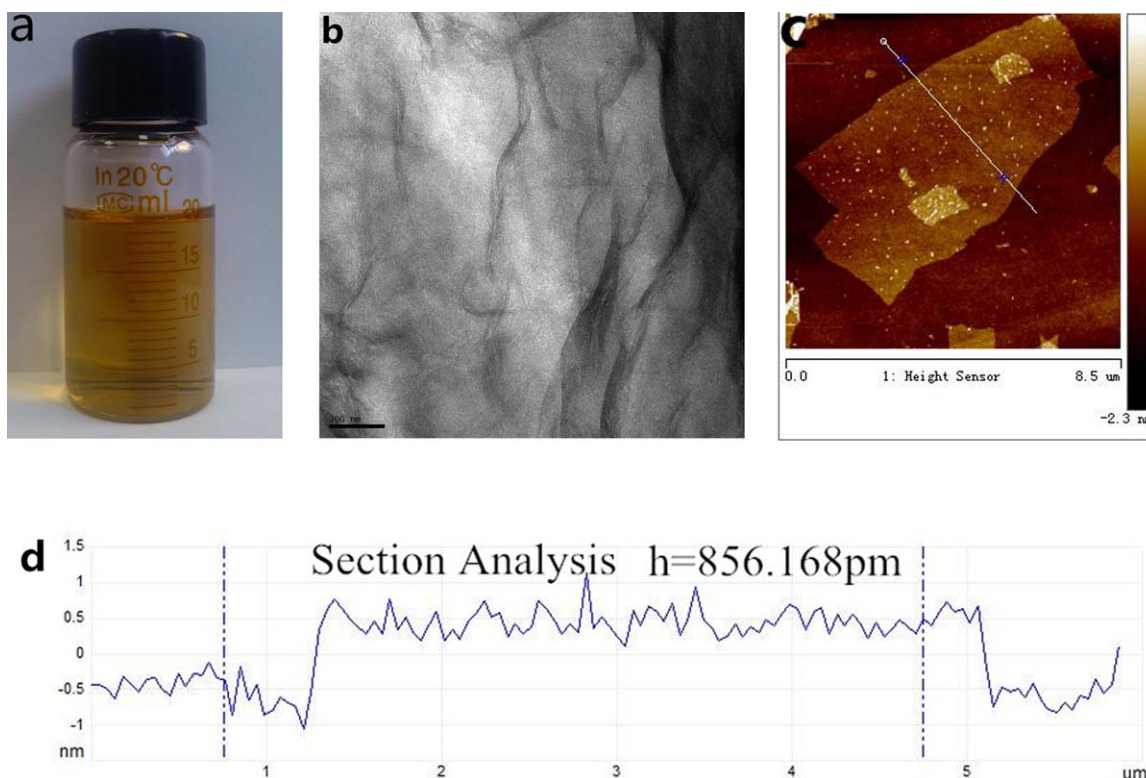


Figure 2. Dispersion of GO in water (a), TEM image of GO sheets (b), AFM image of GO sheets (c), and cross-section analysis of GO sheets (d). [Color figure can be viewed in the online issue, which is available at wileyonlinelibrary.com.]

Characterizations

The morphology property of GO sheets was performed on a Dimension Icon type atomic force microscope (AFM) system (Bruker, USA) and a JEM 2010 transmission electron microscopy (TEM) (Electronics, Japan). Fourier transform infrared (FTIR) measurements were conducted on a Nicolet 380 infrared spectrometer (Thermo Electron Corporation, United States). The scanning electron microscopy (SEM) (FEI, USA) images were gained on a FEI QUANTA FEG 250 field emission SEM system.

Particle size and distribution of the sizing agent were tested by a LS-13320 dynamic laser particle analyzer (Beckman Coulter, United States) using the polarization intensity differential scattering technology (PIDS) at 25°C. The mean diameter of the particles was determined by the software provided by Beckman Coulter instrument. Zeta potentials of the sizing agents were measured by JS9H type electrophoresis apparatus (Shanghai Zhongchen Digital Technology Equipment, China).

Abrasion resistance was tested by LFY-109B fiber abrasion tester (Shandong Textile Academy, China).³⁷ Fluffs and breakage was measured according to Japanese patent.³⁸ Unwinding carbon bundle fiber was obtained according to ISO 3375-2009 standard. The stainless steel hook (radius of 10 mm) was made of a stick (radius of 5 mm). There was a sliding scale at standard distance of 60 mm below the suspension point.²

Three-point short beam shear test was used to determine the interlaminar shear strength (ILSS) values of CF-reinforced composites according to ASTM D-2344² test standard. The specimens were prepared by resin-transfer molding (RTM). The

poured resin was epoxy resin E-51, and the curing agent was TETA. The mass ratio of E-51 to TETA was 100 : 15. The specimens were unidirectional CF/epoxy resin composites with 30% volume content of CF. The dimensions of the specimens for the short beam shear test were 20 mm × 6 mm × 3 mm. The test was carried out in a WDW-30 type universal testing machine (Shanghai Shenli Testing Machine, China) using a cross-head speed of 1 mm/min. Ten specimens for every type of composite were measured and the ILSS value was calculated according to the following equation:

$$\text{ILSS} = 3P_b/4bh \quad (1)$$

where P_b is the failure load, b and h are the specimen width and thickness, respectively.

RESULTS AND DISCUSSION

Morphology and Structure of GO Sheets

In contrast to black hydrophobic graphite, GO suspension (1 mg/mL) exhibits a slight golden color [as shown in the digital photo, Figure 2(a)]. The hydrophilic groups (carboxyl and hydroxyl groups) were introduced into the edge sites through an oxidation process, which guaranteed the stable existence in aqueous medium.³⁴ TEM analysis shows that the GO sheets appear typically flat yet wrinkled [Figure 2(b)]. A representative AFM image of GO sheets is shown in Figure 2(c,d), which reveals the presence of irregularly shaped sheets with uniform thickness. As indicated in Figure 2(c) for the part marked by the white line, the thickness of the sheet is typically 1.0 nm, which is in good agreement with previous reported single-layer



Figure 3. Schematic illustration of graphite by oxidation. [Color figure can be viewed in the online issue, which is available at wileyonlinelibrary.com.]

GO sheets.^{39–41} This observation leads to a conclusion that complete exfoliation of graphite oxide down to individual GO sheet was indeed achieved. Figure 3 shows the schematic illustration of graphite oxidation and exfoliation.

The Chemical Structure of Graphite, GO, Epoxy Resin, and TETA

The obtained materials were characterized by FT-IR, as shown in Figure 4. In Figure 4(a), for GO, the peaks at 1053 and 1220 cm^{-1} show the presence of epoxy C-O. The characteristic peaks at 1737 and 1623 cm^{-1} appear for carboxyl C=O and aromatic C=C, respectively. For graphite, there is no peak existence. This demonstrates that the hydrophilic groups (carboxyl and hydroxyl groups) have been introduced into the edge sites successfully through the oxidation process. The chemical structure of epoxy matrix and TETA are shown in Figure 4(b). For epoxy resin, the peaks at 841 and 920 cm^{-1} are attributed to stretching vibration of C-O-C and C-O of oxirane group, respectively. The peak at 1040 cm^{-1} belongs to stretching vibration of C-O-C of ethers. The peak at 2950 cm^{-1} is designed as stretching vibration of C-H. For TETA, the peaks at 839, 1620 cm^{-1} , and 3370 cm^{-1} are designed as out of plane bending vibration, in-plane bending vibration and stretching vibration of N-H, respectively. The peaks at 1080 and 1130 cm^{-1} show the presence of C-N stretching vibrations. The chemical structure of GO, epoxy resin, and TETA will be conducive to explaining the mechanism of ILSS of unidirectional CF/epoxy composites.

Properties of the Sizing Agents

Figure 5 shows the different phenomena of the three sizing agents standing 3 days later. A amount of resin precipitation could be noticed from the bottom of SA-3. Both SA-1 and SA-2 could maintain no obvious precipitation after more than one month, while SA-3 got failed 3 days later, which meant that SA-1 and SA-2 sizing agents had the superior stability than SA-3. As for SA-3 sizing agent, there were not enough emulsifier

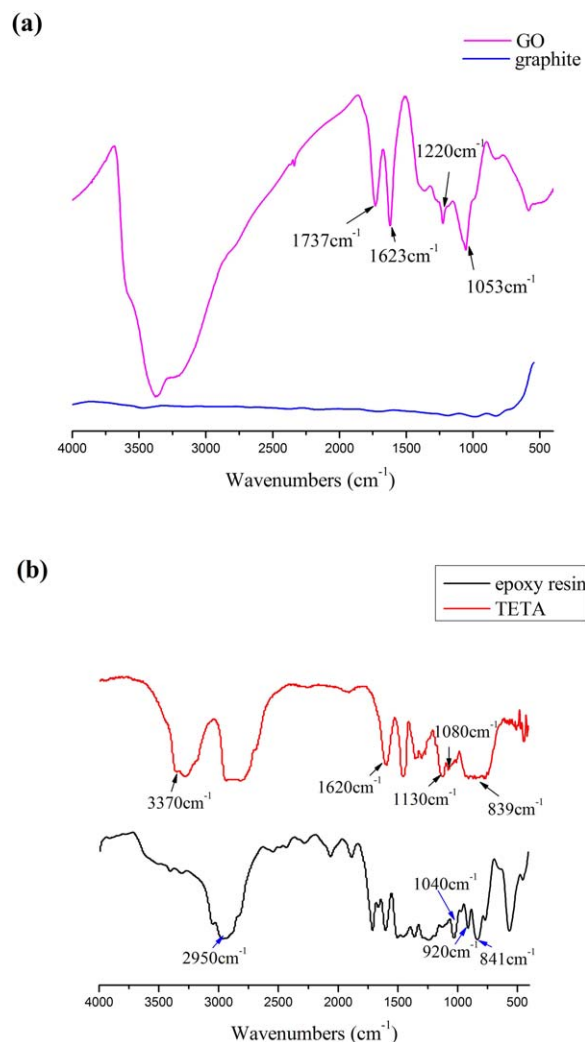


Figure 4. The FTIR spectra: (a) GO and graphite and (b) epoxy matrix

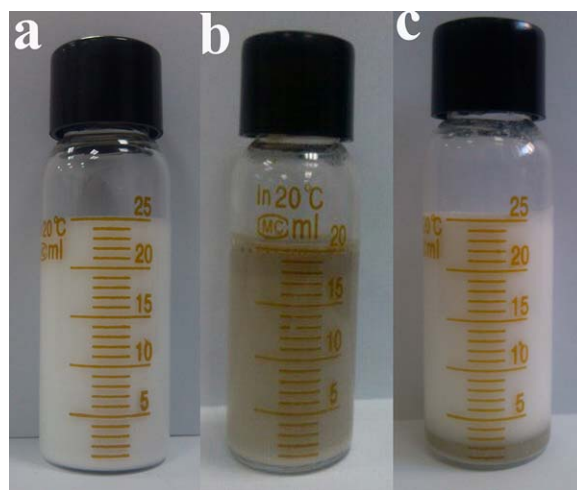


Figure 5. The three sizing agents after 3 days later: (a) SA-1 sizing agent, (b) SA-2 sizing agent, and (c) SA-3 sizing agent (have a layer of resin precipitation at a bottom of bottle). [Color figure can be viewed in the online issue, which is available at wileyonlinelibrary.com.]

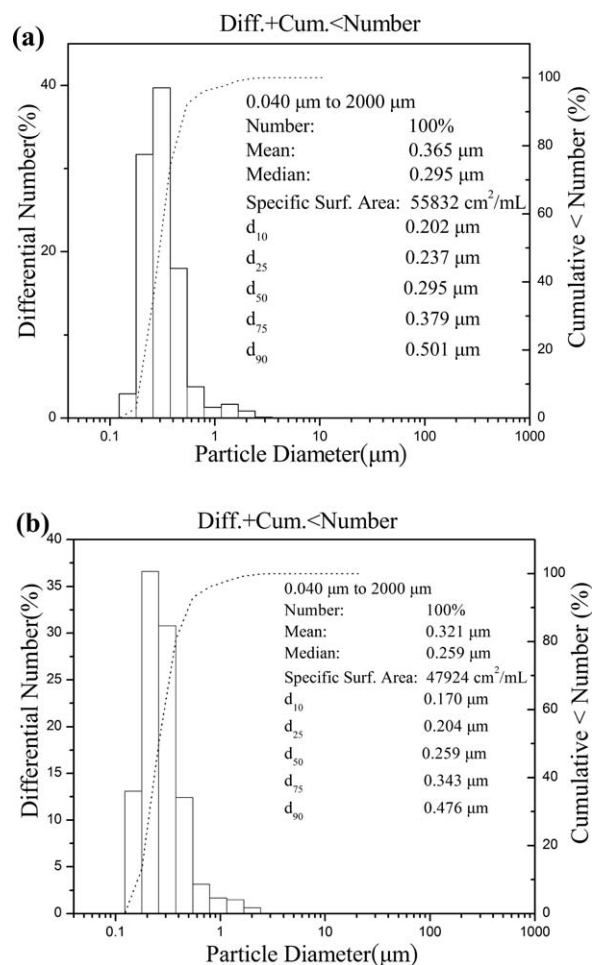


Figure 6. The particle size and distribution of the emulsions: (a) SA-1 sizing agent, and (b) SA-2 sizing agent.

molecules on the surface to pack the water drops. Therefore, small water drops tended to collide with each other and form big drops when they were suffered with high shear stirring. When water drops dispersed randomly in system, incomplete phase inversion was formed, which led to unstable system and obvious precipitation of the emulsion. However, as for SA-1 and SA-2 sizing agents, the emulsifier molecules or GO sheets were enough to pack water drops and strong interfacial film was formed subsequently. The interfacial film was strong enough to make oil phase (resin phase) isolated. The resin droplets with less chance combined to each other. At this state the system was easy to form complete phase inversion. Therefore, the stable emulsions were obtained.

To make further investigation on the stability of the SA-1 and SA-2, a dynamic laser particle analyzer was employed to examine their particle sizes and distributions. It is well known that, as for an emulsion, the first parameter to be taken into consideration is the particle size. According to the Stoke Law,⁴² the smaller the particles are, the more stable the emulsion is. Moreover, an emulsion sizing with a smaller mean particle diameter usually possesses a better ability of film formation and is beneficial to the interfacial adhesion of composite.⁸ As shown in Figure 6, the mean particle size of SA-1 and SA-2 are 365 and

321 nm, respectively. Therefore, the particle size distribution of SA-2 sizing agent is narrower and more stable than SA-1 sizing agent.

The stability and aggregation of dispersions are affected by the zeta potential of those colloidal dispersions.⁴³ The zeta potential can be used to investigate how charged particles affect the behavior of the dispersion such as aggregation, flow, sedimentation, and filtration.⁴³ When the magnitude of the potential is small, attraction exceeds repulsion and the dispersion will break and flocculate. Therefore, zeta potentials of SA-1 and SA-2 were investigated. The tested results of the zeta potential of the SA-1 and SA-2 were -21.56 and -64.19 mV, respectively, which showed that droplets of the SA-2 could not easily aggregate because of the powerful repulsion exceeding attraction. The aspect contributes to revealing that the SA-2 sizing agent was more stable.

Synthetically, the particle size and distribution and zeta potential could reflect that a satisfactory stability of the SA-2.

From the above points of view, it was noticed that GO sheets played a very important role in the stable emulsion. The process of emulsification along with GO absorption process at the interface of the two immiscible liquids led to a reduction in the free energy of the system. The high surface area of GO sheets enabled them to be trapped at the interface and to wrap around the oil droplets.³¹

Surface Topography of Modified CF

The SEM morphologies of SA-1 sized CF, desized CF, and SA-2 sized CF are shown in Figure 7. As shown in Figure 7(a), CF sized by SA-1 sizing agent has the smooth surface and slight convex hills. In Figure 7(b), longitudinal grooves uniformly disperse on desized CF surface. However, after sized with the Pickering emulsion type sizing agent, CF surface was covered with GO sheets [Figure 7(c)]. The surface of sized CF becomes smooth and the longitudinal grooves become shallower because of longitudinal grooves and flaws filled with sizing agents during sizing process. Figure 7(d) is a higher magnification of Figure 7(c). This indicates that after different treatments the surface topography of CF has been changed. The Pickering emulsion obviously changed the surface topography of CF.^{44,45}

Handling Characteristics

The results in Table II clearly demonstrate that the SA-1 sizing agent and SA-2 sizing agent stabilized by GO sheets could greatly improve the workability of CF. It means that sizing agent could serve as a lubricant to protect fiber and facilitate handling processing during subsequent textile processing.³²

Among them, CF sized by the SA-1 has the maximum abrasion resistance, which reaches about 2186 times. The CF sized with the SA-2 goes near to the abrasion times of the SA-1 sized CF and reaches about 2108 times. Wear resistance of CF could be explained by fluffs and breakage. GO sheets coated onto the surface increased the surface roughness and fluffs of CF, which resulted in decreasing abrasion resistance.

The stiffness value of desized CF is lowest, 23 mm. The stiffness values of CF sized by different sizing formula are almost the

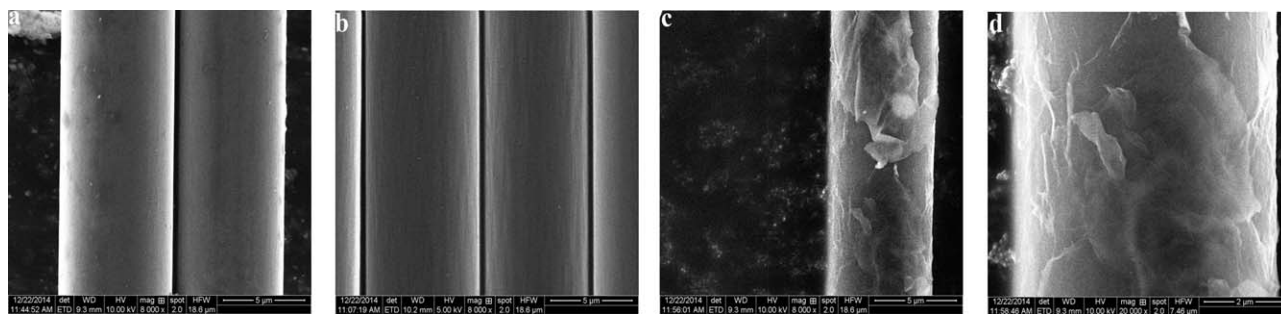


Figure 7. SEM images of the CF after sizing treatment: (a) CF sized by SA-1 sizing agent; (b) Desized CF; (c) CF sized by SA-2 sizing agent; and (d) A higher magnification of (c).

same, around 64 mm. The small difference between the specimens might result from the toughening effect on the surface of GO sheets. Stiffness could reflect the flexibility of CF bundle. CF will be bended frequently during process of weaving the tows to fabrics, so, appropriate flexibility for CF is required. Generally, the higher the stiffness is, the lower the flexibility is. CF sized by SA-1 and SA-2 have the appropriate stiffness.

From the above analysis, it can be concluded that CF bundle sized by SA-2 conforms to the requirement of CF handling characteristics during subsequent textile processing.

ILSS of Unidirectional CF/Epoxy Composites

The mechanical property of CF-reinforced polymer composite is, to a large extent, controlled by the interfacial adhesion between the fiber and matrix. ILSS is one of the most important indicators of interfacial adhesion in composite. Figure 8 shows the ILSS values of CF reinforced composites. As a comparison, the aqueous dispersion of GO was directly added into SA-1 epoxy emulsion and then CF was sized to get its composite. In this work, the weight of GO was the same as the SA-2 sizing agent. The sizing agent sample was marked as SA-4. The ILSS of the desized CF composite, the SA-1 sized CF composite, the SA-2 sized CF composite and the SA-4 sized CF composite are 34.05, 40.15, 44.67, and 42.89 MPa, respectively. The ILSS of the CF composite sized by SA-2 sizing agent is the highest, increasing by 31.19%, 11.26%, and 4.15%, respectively, compared with that of the ILSS values of desized CF composites, sized by SA-1 and SA-4, respectively. It indicates that the type of sizing agent had affected the interfacial performance of composites.

The exact mechanism of the ILSS improvement of the SA-2 sized CF composite could be explained through interfacial microstruc-

ture and chemical bonding between GO sheets and the matrix resin. As shown in Figure 7(c), the CF sized by SA-2 had the wrinkled and roughened textures which might increase the wettability between CF and the matrix. As for chemical bonding, firstly, when the CF was sized by SA-2, the functional groups of GO surface, such as hydroxyl groups and carboxyl groups could react with epoxy groups and helped to form chemical combination between GO sheets and the matrix. Secondly, GO containing pendant oxygen-containing groups might form strong hydrogen bonds with the oxygen groups of epoxy resin. Thirdly, TETA as a curing agent could connect GO sheets and epoxy matrix in the interfacial region through the reaction between epoxy groups.³³ Finally, The “crack-tip bridging”⁴⁶ and “gradient interphase”⁴⁷ effects were also important reasons for the ILSS values improvement. The relevant chemical structure of GO, epoxy resin, and TETA are presented in Figure 4. Meanwhile, the relevant reactions in the interface region are shown in Figure 9(a,b).

However, the ILSS of CF reinforced composite sized by SA-4 sizing agent has a little decrease compared with that of sized by SA-2 sizing agent. After CF sized with the SA-2 sizing agent, GO sheets were evenly adhered on the CF surface. The mass ratio of emulsifiers/resin for SA-1 sizing agent was 10% which had been reached saturation. The extra addition of GO could not stabilize on the interface between oil and water and directly dissolve in water phase. When the CF was sized by SA-4, GO

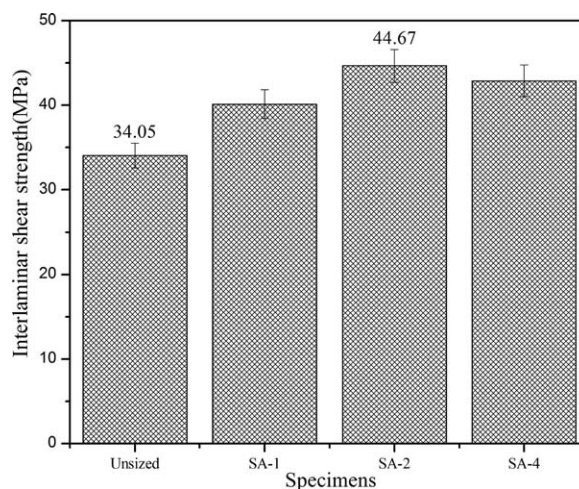


Figure 8. The ILSS of unidirectional CF/epoxy composites.

Table II. Handling Characteristics of Different Types CF

| samples | Handling characteristics | | |
|---------------|-----------------------------|--------------------------|----------------------|
| | abrasion resistance (times) | fluffs and breakage (mg) | stiffness value (mm) |
| Desized CF | 1093 ± 49 | 11.7 ± 0.3 | 23 ± 3 |
| SA-1 sized CF | 2171 ± 96 | 3.2 ± 0.2 | 64 ± 1 |
| SA-2 sized CF | 2108 ± 90 | 3.5 ± 0.1 | 65 ± 2 |

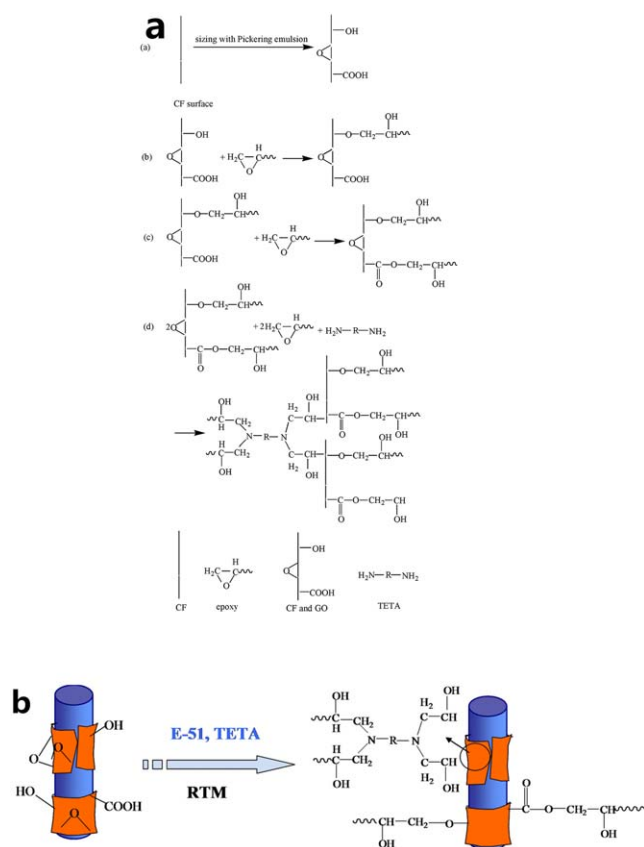


Figure 9. The interface region reactions: (a) Chemical reaction equations; (b) Schematic illustration of the interface reactions. [Color figure can be viewed in the online issue, which is available at wileyonlinelibrary.com.]

sheets were unable to adhere onto the CF surface homogeneously. Thereby, the effects of the delayed crack opening and the reduced interlaminar stress concentration were smaller than SA-2. In turn the ILSS value of its composite was lower than the SA-2 sized CF composite.

Micrographs of Fracture Surfaces

Further studies on the interfacial properties for both the desized and the SA-2 sized CF composites were carried out by observing

the fracture surfaces morphology of the composites after the ILSS tests. SEM images of the fracture surfaces of the fractured composites are shown in Figure 10. As for the desized CF/epoxy resin composite [Figure 10(a)], there is little residual epoxy resin adhering on the CF surface because of the poor CF/epoxy resin interfacial adhesion. On the contrary, for SA-2 sizing agent sized CF composite, a significantly different interface microstructure is shown in Figure 10(b). In addition to lesser fiber extraction, a considerable plastic deformation and an amount of resin adhering to the CFs surface can be seen on the fractograph. The development of the microstructure should be related to the interaction between the GO sheets and epoxy resin. This is responsible for the improvement of ILSS.

CONCLUSIONS

By using GO sheets and surfactants as the mixed emulsifier system, the Pickering emulsion sizing agent was successfully prepared through phase inversion emulsification method. The method was not only cost saving but also environmental friendly. The particle size and distribution of the Pickering emulsion was narrower and more stable than that of SA-1 sizing agent. It indicated that the properties of the Pickering emulsion were better than SA-1 sizing agent simply stabilized by a mass of surfactants. The key factor for the stability of the Pickering emulsion was that the high surface area of GO sheets enabled them to be trapped at the interface and to wrap around the oil droplets decreasing the particle size. SEM images showed that there existed a layer of sizing agent film with GO sheets evenly on the CF surface after the CF was sized. The abrasion resistance of the CF sized by the Pickering emulsion reached 2108 times and the stiffness was 65 mm, demonstrating a greatly enhanced handleability of CF bundle compared with those of the desized one (1093 time, 23 mm). The ILSS of the composite with the CF sized by the Pickering emulsion sizing agent reached about 44.67 MPa, achieving 31.19% and 11.26% improvement, respectively, compared with the ILSS values of desized CF composite and SA-1 CF composite, respectively. Its fracture section was more compact and the CF debonding was more difficult. It indicated that the stronger adhesion was existence between CF and epoxy resin. The potential chemical

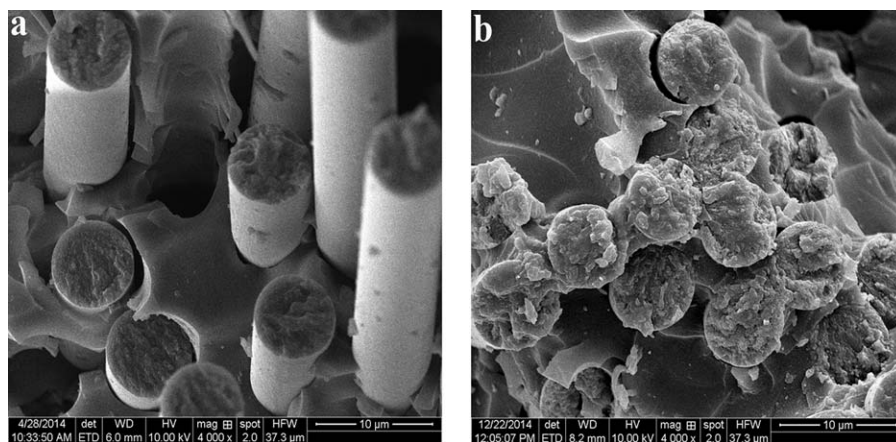


Figure 10. Fracture surface micrographs of CF/epoxy composites: (a) Desized CF composite, (b) CF composite sized by SA-2 sizing agent.

reactions between the matrix and the GO sheets as well as the better wettability of CF and hydrogen bonding might contribute to improving the interfacial strength. This work provides an ingenious and effective method to fabricate a potential and excellent CF composite with good interfacial property.

ACKNOWLEDGMENTS

The authors sincerely acknowledge the financial support from the Science and Technology Program of the Higher Education Institutions of Shandong Province (J13LA06) and Special Plan for Independent Innovation and Achievements Transformation of Shandong Province, China (Grant No. 2014ZZCX05302).

REFERENCES

1. An, F.; Lu, C. X.; Li, Y. H.; Guo, J. H.; Lu, X. X.; Lu, H. B.; He, S. Q.; Yang, Y. *Mater. Des.* **2012**, *33*, 197.
2. Liu, J. Y.; Ge, H. Y.; Chen, J.; Wang, D. Z.; Liu, H. S. *J. Appl. Polym. Sci.* **2012**, *124*, 864.
3. Montes-Morán, M. A.; Gauthier, W.; Martínez-Alonso, A.; Tascón, J. M. D. *Carbon* **2004**, *42*, 1275.
4. Bakkar, A.; Neubert, V. *Electrochim. Acta* **2009**, *54*, 1597.
5. Karsli, N. G.; Aytac, A. *Compos. Part B* **2013**, *51*, 270.
6. Dilsiz, N.; Wightman, J. P. *Colloids Surf. A* **2000**, *164*, 325.
7. Dai, Z. S.; Shi, F. H.; Zhang, B. Y.; Li, M.; Zhang, Z. G. *Appl. Surf. Sci.* **2011**, *257*, 6980.
8. Zhang, R. L.; Liu, Y.; Huang, Y. D.; Liu, L. *Appl. Surf. Sci.* **2013**, *287*, 423.
9. Huang, H.; You, B.; Zhou, S. X.; Wu, L. M. *J. Colloid Interface Sci.* **2007**, *310*, 121.
10. Nam, Y. S.; Kim, J. W.; Park, J. Y.; Shim, J. W.; Lee, J. S.; Han, S. H. *Colloids Surf. B* **2012**, *94*, 51.
11. Pickering, S. U. *J. Chem. Soc. Perkin Trans.* **1907**, *91*, 2001.
12. Tcholakova, S.; Denkov, N. D.; Lips, A. *Phys. Chem. Chem. Phys.* **2008**, *10*, 1608.
13. Binks, B. P. *Curr. Opin. Colloid Interface Sci.* **2002**, *7*, 21.
14. Aveyard, R.; Binks, B. P.; and Clint, J. H. *Adv. Colloid Interface Sci.* **2003**, *100*, 503.
15. Yan, N.; Gray, M. R.; Masliyah, J. H. *Colloids Surf. A* **2001**, *193*, 97.
16. Lan, Q.; Yang, F.; Zhang, S. Y.; Liu, S. Y.; Xu, J.; Sun, D. *J. Colloids Surf. A* **2007**, *302*, 126.
17. Li, C. E.; Zhang, S. Y.; Wang, J. *Acta Chim. Sin.* **2008**, *66*, 2313.
18. Dickinson, E. *Curr. Opin. Colloid Interface Sci.* **2010**, *15*, 40.
19. Frelichowska, J.; Bolzinger, M. A.; Pelletier, J.; Valour, J. P.; Chevalier, Y. *Int. J. Pharm.* **2009**, *371*, 56.
20. Pedrazzoli, D.; Pegoretti, A. *Compos. Sci. Technol.* **2013**, *76*, 77.
21. Fang, C. Q.; Wang, J. L.; Zhang, T. *Appl. Surf. Sci.* **2014**, *321*, 1.
22. Meyer, J. C.; Geim, A. K.; Katsnelson, M. I.; Novoselov, K. S.; Booth, T. J.; Roth, S. *Nature* **2007**, *446*, 60.
23. Hassan, M.; Reddy, K. R.; Haque, E.; Faisal, S. N.; Ghasemi, S.; Minett, A. I.; Gomes, V. G. *Compos. Sci. Technol.* **2014**, *98*, 1.
24. Thomassin, J. M.; Trifkovic, M.; Alkarmo, W.; Detrembleur, C.; Jérôme, C.; Macosko, C. *Macromolecules* **2014**, *47*, 2149.
25. Morimune, S.; Kotera, M.; Nishino, T.; Goto, T. *Carbon* **2014**, *70*, 38.
26. Hassan, M.; Reddy, K. R.; Haque, E.; Minett, A. I.; Gomes, V. G. *J. Colloid Interface Sci.* **2013**, *410*, 43.
27. Lee, Y. R.; Kim, S. C.; Lee, H. I.; Jeong, H. M.; Raghu, A. V.; Reddy, K. R.; Kim, B. K. *Macromol. Res.* **2011**, *19*, 66.
28. Han, S. J.; Lee, H. I.; Jeong, H. M.; Kim, B. K.; Raghu, A. V.; Reddy, K. R. *J. Macromol. Sci. B* **2014**, *53*, 1193.
29. Moon, I. K.; Lee, J.; Ruoff, R. S.; Lee, H. *Nat. Commun.* **2010**, *1*, 73.
30. Wang, S. R.; Zhang, Y.; Abidi, N.; Cabrales, L. *Langmuir* **2009**, *25*, 11078.
31. He, Y. Q.; Wu, F.; Sun, X. Y.; Li, R. Q.; Guo, Y. Q.; Li, C. B.; Zhang, L.; Xing, F. B.; Wang, W.; Gao, J. P. *ACS Appl. Mater. Interfaces* **2013**, *5*, 4843.
32. Chen, J.; Zhou, X. R.; Ge, H. Y.; Wang, D. Z.; Liu, H. S.; Li, S. *Polym. Compos.* **2014**, DOI: 10.1002/pc.23185.
33. Zhang, X. Q.; Fan, X. Y.; Yan, C.; Li, H. Z.; Zhu, Y. D.; Li, X. T.; Yu, L. P. *ACS Appl. Mater. Interfaces* **2012**, *4*, 1543.
34. Chen, J.; Zhao, D.; Jin, X.; Wang, C. C.; Wang, D. Z.; Ge, H. Y. *Compos. Sci. Technol.* **2014**, *97*, 41.
35. Kim, M. T.; Kim, M. H.; Rhee, K. Y.; Park, S. *J. Compos. Part B* **2011**, *42*, 499.
36. Hatsuo, I.; Thanyalak, C. *Polym. Compos.* **2003**, *24*, 597.
37. Ge, H. Y.; Li, S.; Wang, D. Z.; Chen, J. *J. Appl. Polym. Sci.* **2014**, *131*, 39843.
38. Isao, N. Japan Patent. 10-266076, **1998**.
39. Stankovich, S.; Dikin, D. A.; Piner, R. D.; Kohlhaas, K. A.; Kleinhammes, A.; Jia, Y.; Wu, Y.; Nguyen, S. T.; Ruoff, R. S. *Carbon* **2007**, *45*, 1558.
40. Stankovich, S.; Dikin, D. A.; Dommett, G. H. B.; Kohlhaas, K. M.; Zimney, E. J.; Stach, E. A.; Piner, R. D.; Nguyen, S. T.; Ruoff, R. S. *Nature* **2006**, *442*, 282.
41. Gomez-Navarro, C.; Burghard, M.; Kern, K. *Nano Lett.* **2008**, *8*, 2045.
42. Liu, J. Y. Thesis, University of Jinan, **2012**.
43. Bremmel, K. E.; Jameson, G. J.; Biggs, S. *Colloids Surf. A* **1999**, *146*, 75.
44. Ou, J. F.; Wang, J. Q.; Liu, S.; Mu, B.; Ren, J. F.; Wang, H. G.; Yang, S. G. *Langmuir* **2010**, *26*, 15830.
45. Tang, H.; Ehlert, G. J.; Lin, Y.; Sodano, H. A. *Nano Lett.* **2011**, *12*, 84.
46. Siddiqui, N. A.; Sham, M. L.; Tang, B. Z.; Munir, A.; Kim, J. K. *Compos. Part A* **2009**, *40*, 1606.
47. Chen, L.; Jin, H.; Xu, Z. W.; Shan, M. J.; Tian, X.; Yang, C. Y.; Wang, Z.; Cheng, B. W. *Mater. Chem. Phys.* **2014**, *145*, 186.